



# Magneto-elastic phase transition in a linear chain within the double and super-exchange model

J.R. Suárez<sup>a,\*</sup>, E. Vallejo<sup>a</sup>, O. Navarro<sup>a</sup>, M. Avignon<sup>b</sup>

<sup>a</sup> Instituto de Investigaciones en Materiales, Universidad Nacional Autónoma de México, Apartado Postal 70-360, 04510 México D.F., Mexico

<sup>b</sup> Institut Néel, Centre National de la Recherche Scientifique (CNRS) and Université Joseph Fourier, BP 166, 38042 Grenoble Cedex 9, France

## ARTICLE INFO

Available online 27 May 2009

### Keywords:

Double and super-exchange interaction  
Classical spin model  
Phase separation

## ABSTRACT

In this work a magneto-elastic phase transition in a linear chain was obtained due the interplay between magnetism and lattice distortion in a double and super-exchange model. We consider a linear chain consisting of classical localized spins interacting with itinerant electrons. Due to the double exchange interaction, localized spins align ferromagnetically. This ferromagnetic tendency is expected to be frustrated by the anti-ferromagnetic super-exchange interaction between neighbor localized spins. Additionally, the lattice parameter is allowed to have small changes, which contributes harmonically to the energy of the system. The phase diagram is obtained as a function of the electron density and the super-exchange interaction using a Monte Carlo minimization. At low super-exchange interaction energy phase transition between electron-full ferromagnetic distorted and electron-empty anti-ferromagnetic undistorted phases occurs. In this case all electrons and lattice distortions were found within the ferromagnetic domain. For high super-exchange interaction energy, phase transition between two site distorted periodic arrangement of independent magnetic polarons ordered anti-ferromagnetically and the electron-empty anti-ferromagnetic undistorted phase was found. For this high interaction energy, Wigner crystallization, lattice distortion and charge distribution inside two-site polarons were obtained.

© 2009 Elsevier B.V. All rights reserved.

## 1. Introduction

Physics of transition-metal oxides has revealed a variety of phenomena in the last decades [1]. Among those phenomena, colossal magnetoresistance has attracted much interest not only as a challenging subject of fundamental science but also as an important phenomenon for potential spintronic applications. Typically, the materials that present this phenomenon have a perovskite-type lattice structure and display a broad spectrum of physical properties depending on filling, temperature and other parameters. Theoretical studies concentrate their efforts to explain the colossal magnetoresistance and the half-metallic behavior observed in the ferromagnetic phase of manganese oxides [2] and in double perovskites [3], respectively. For these studies the so-called double exchange (DE) model was used. The DE mechanism was early introduced by Zener [4]. The origin of such mechanism lies in the intra-atomic Hund's spin coupling  $J_H$ , of localized electrons with itinerant electrons. DE mechanism has been widely used in the context of manganites [4–6]. The DE model explain how carriers improve their kinetic energy by forcing the localized spins to become ferromagnetically ordered. This ferromagnetic (F) tendency is expected to be frustrated by

anti-ferromagnetic (AF) super-exchange (SE) interactions between localized spins  $\vec{S}_i$  as first discussed by de Gennes [7] who conjectured the existence of canted states. In spite of recent interesting advances, our knowledge of spin and charge ordering resulting from the competition between DE and SE interactions is still incomplete.

Recently, it has been shown that three-leg ladders in the oxyborate system  $\text{Fe}_3\text{BO}_5$  may provide evidence for the existence of spin and charge ordering resulting from such a competition [8]. The former Fe-oxyborate known as Fe-ludwigite contains subunits in the form of three-leg ladders of Fe cations and presents an interesting structural and charge ordering transition at  $T_c \approx 283$  K, such long and short bonds on the rungs alternate along the ladder axis [9].

The main goal of this work will be to study the interplay between magnetic interactions and lattice distortion in one-dimensional systems. A double and super-exchange model will be used together with a lattice distortion. This model leads to a magneto-elastic phase transition and lattice contraction that consequently change the lattice parameters. The lattice parameters change could be detectable using neutron diffraction techniques as in  $\text{La}_2\text{CuO}_{4+\delta}$  [10]. The contraction obtained in this work can be related to the contraction of the rungs experimentally observed using X-ray diffraction studies in the Fe-ludwigite [11].

The double-exchange Hamiltonian, in the strong coupling limit  $J_H \rightarrow \infty$ , a limit commonly called itself the DE model, takes the

\* Corresponding author. Tel.: +52 443 3223897.

E-mail address: [jrsuarez@iim.unam.mx](mailto:jrsuarez@iim.unam.mx) (J.R. Suárez).

well-known form

$$H = - \sum_i t_{i,i+1} \cos\left(\frac{\theta_{i,i+1}}{2}\right) (c_i^\dagger c_{i+1} + h.c.), \quad (1)$$

where  $c_{i\sigma}^\dagger (c_{i\sigma})$  are the fermion creation (annihilation) operators of conduction electrons at site  $i$  with spin  $\sigma$  and  $t_{i,i+1}$  is the hopping parameter. Because of the strong Hund's coupling limit itinerant electrons are now either parallel or antiparallel to the local spins.  $\theta_{i,i+1}$  is the relative angle between the classical localized spins at sites  $i$  and  $i + 1$  which are specified by their polar angles  $\phi_i$  and  $\varphi_i$ , defined with respect to a  $z$ -axis taken as the spin quantization axis of the itinerant electrons. The SE coupling is an AF inter-atomic exchange coupling between localized spins  $\vec{S}_i$ . We consider local spins as classical  $\vec{S}_i \rightarrow \infty$ , a reasonable approximation in many cases in view of the similarity of the known results [12,13]. Additionally, the effect of lattice distortion will be considered. In our approach, the complicated inter-atomic potential will be represented using classical springs to join the localized atoms. The spring forces are assumed to be linear (small displacements, Hooke's law). The hopping term changes as  $t_{i,i+1} = t(1 + \delta_{i,i+1})$  with  $-1 \ll \delta_{i,i+1} \ll 1$  being  $\delta_{i,i+1}$  the  $(i, i + 1)$ -spring displacement because of lattice distortion. The complete Hamiltonian in the nearest-neighbor limit is given by

$$H = -t \sum_i (1 + \delta_{i,i+1}) \cos\left(\frac{\theta_{i,i+1}}{2}\right) (c_i^\dagger c_{i+1} + h.c.) + JS^2 \sum_i \cos(\theta_{i,i+1}) + B \sum_i \delta_{i,i+1}^2. \quad (2)$$

$J$  and  $B$  are SE interaction and elastic energies, respectively.

## 2. Results and discussion

The phase diagram of this model was obtained at  $T = 0$  K by using open boundary conditions on a linear chain of  $N = 24$  sites. For a given conduction electron density  $x$  ( $0 \leq x \leq 0.5$  because of hole–electron symmetry), an SE interaction energy and an elastic energy,  $N - 1$  angles ( $\theta_{i,i+1}$ ) and  $N - 1$  spring displacements ( $\delta_{i,i+1}$ ) in the linear chain had to be optimized. For this goal, an analytical

optimization and a classical Monte Carlo method were used. The analytical solution was tested as a starting point in the Monte Carlo simulation. The value  $B/t = 30$  will be taken to guarantee small displacements of all the atoms and consequently a small overall contraction of the chain, for example in the ferromagnetic phase, in which the displacements are present in the whole chain. The magneto-elastic phase diagram obtained here is shown in Fig. 1. For low super-exchange interaction energy,  $JS^2/t \lesssim 0.11$ , an electron-full ferromagnetic distorted (EFD) and an electron-empty anti-ferromagnetic undistorted (EAFU) phase transition was found. Analytical optimization implies angles  $\theta_{i,i+1} = 0$  exactly for the EFD phase. For commensurate electronic fillings at  $x = \frac{1}{3}$  and at  $x = \frac{1}{2}$  (Fig. 2) spring displacements look like Peierls distortion. Because of the typical value of the elastic energy, uniform spring displacements ( $\delta_{ij} = \sin(x\pi)/\pi(B/t)$ ) and uniform charge distribution ( $n_i = x$ ) are expected in the thermodynamic limit ( $N \rightarrow \infty$ ). The  $\delta_{i,i+1} = 0$  spring displacement and  $\theta_{i,i+1} = \pi$  angle solutions were obtained for EAFU phase at  $x = 0$ .

Phase separation (EAFU + EFD in Fig. 1) between EFD and EAFU phases, consist of one large electron-full  $F$  distorted polaron within an electron-empty AF undistorted background. Analytical optimization implies angles 0 and  $\pi$  exactly for the ferromagnetic and anti-ferromagnetic domains, respectively. In the limit  $B/t \rightarrow \infty$ , the magnetic-only F–AF phase transition was previously reported [14].

Above EAFU+EFD phase separation, another phase separation (EAFU + DP3) between  $T$ -phase (for high conduction electron density) and EAFU phase (for  $x = 0$ ) can be observed in Figs. 1 and 3.  $T$ -phase is a more general complex distorted phase found by the Monte Carlo method and can be polaronic like or not. At  $x = \frac{1}{2}$  and  $\frac{1}{3}$   $T$ -phase becomes basically DP2 and DP3 phases, respectively. DP2 and DP3 phases are two and three-site-distorted periodic arrangement of independent  $F$  polarons ordered anti-ferromagnetically. DP2 and DP3 are magneto-elastic Peierls phases. Spring displacements are  $1/2(B/t) \sim 0.0167$  and  $1/2\sqrt{2}(B/t) \sim 0.0118$  for DP2 and DP3 phases, respectively. EAFU + DP3 phase separation is degenerate with phases where the polarons can be ordered or not, while keeping the number of  $F$  and  $AF$  bonds fixed; phases obtained within the “spin-induced Peierls instability” [15] belong

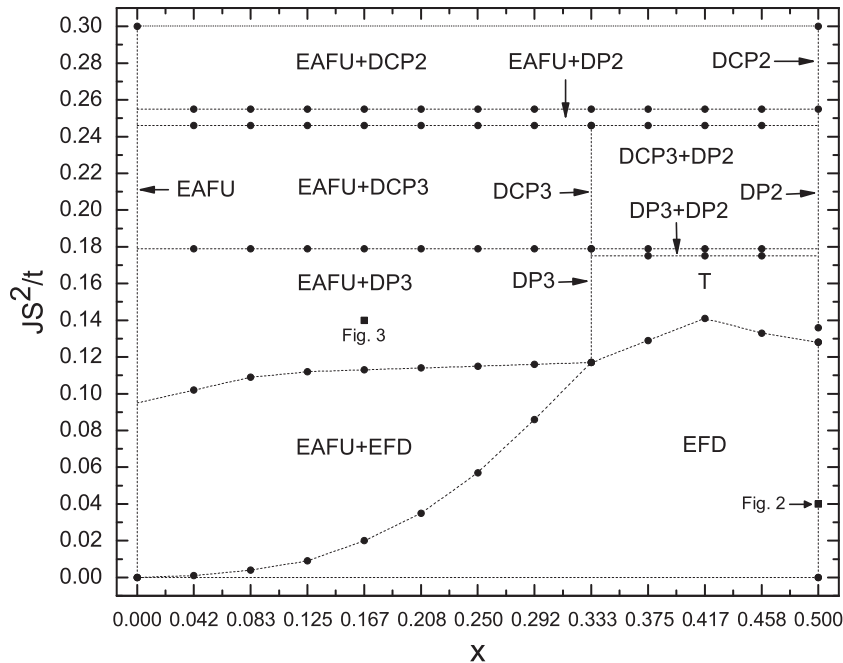
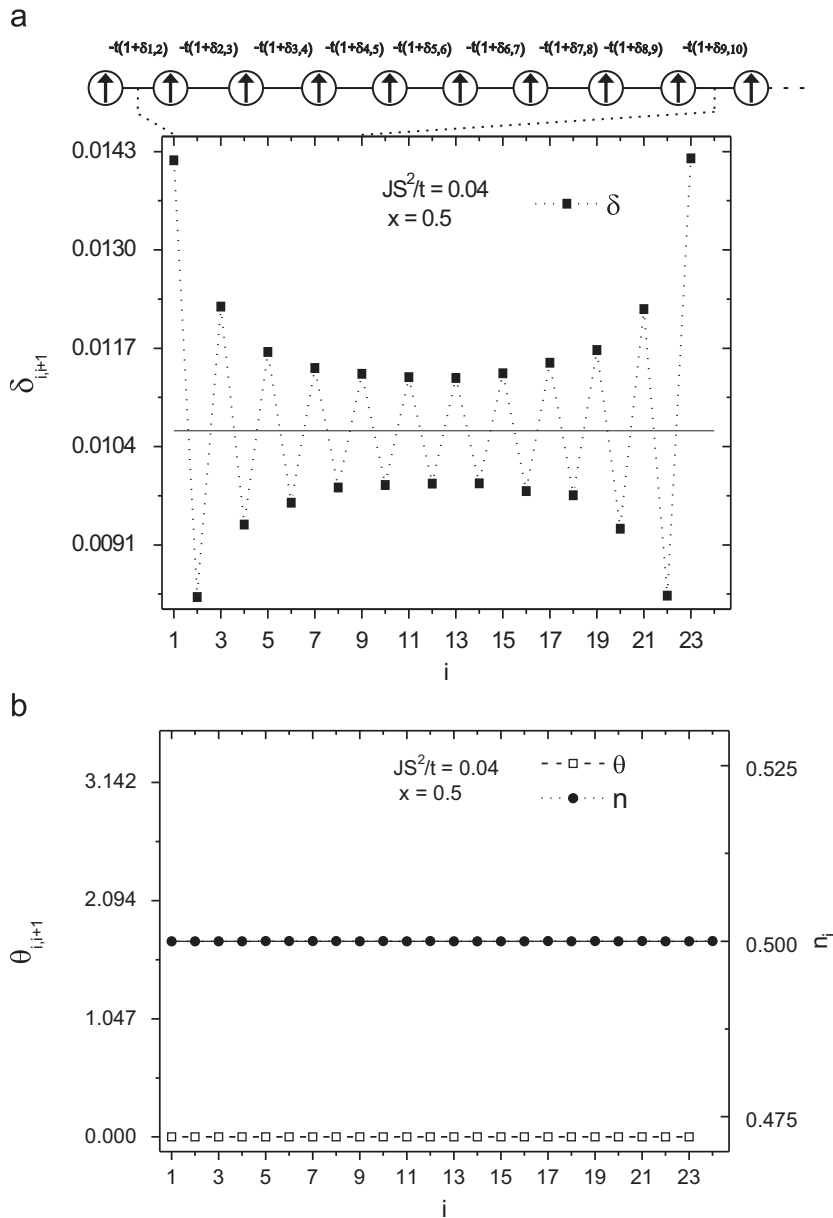


Fig. 1. Magneto-elastic phase diagram as a function of the SE interaction energy  $J$  and the conduction electron density  $x$ , for a typical value of the elastic energy  $B/t = 30$ . A dotted line in this diagram represents a guide for the eyes.



**Fig. 2.** EFD phase for 12 electrons ( $x = 0.5$ ) and  $JS^2/t = 0.04$  showing: (a) spring displacements ( $\delta_{i,i+1}$ ) and (b) angles ( $\theta_{i,i+1}$ ) and charge distribution ( $n_i$ ). Solid lines are: (a) uniform spring displacements and (b) uniform charge distribution obtained for the thermodynamic limit. Partial spin configuration snapshot is also shown.

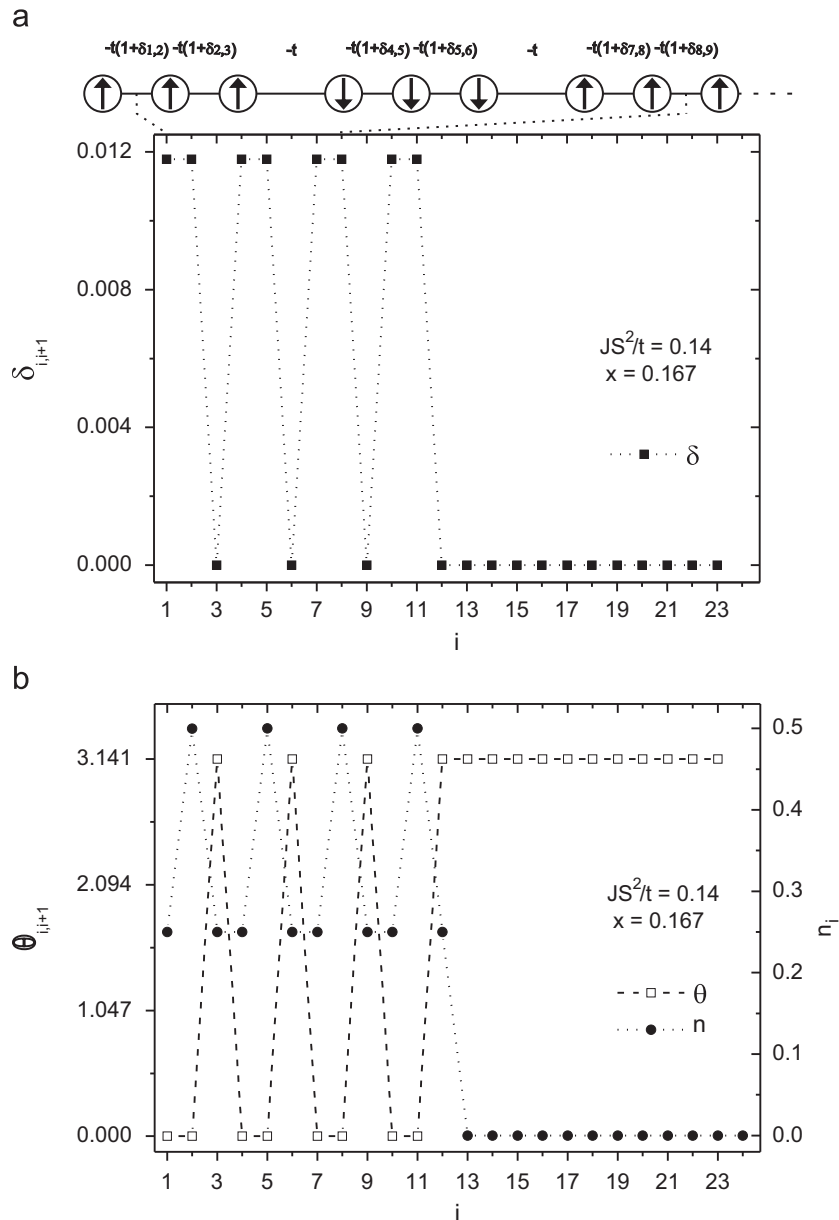
to this class. The former degeneracy unifies ideas like phase separation and individual polarons and gives a natural response to the instability at the Fermi energy and to an infinite compressibility as well. It is worth to notice that in the magnetic-only case, a phase AF + P3 (similar to EAFU + DP3) was identified using  $S = \frac{3}{2}$  quantum spins [16]. P2 and P3 phases were also previously reported for classical [14,15] and  $S = \frac{1}{2}$  quantum [12] local spins.

Fig. 3 shows EAFU + DP3 phase separation for a typical value of the SE interaction energy  $JS^2/t = 0.14$ . As can be seen in this figure, there is a single electron inside each three-site independent magnetic polaron, so a Wigner crystallization is formed. For DP3 and EAFU + DP3 phases, we find lattice distortion within each three-site magnetic polaron.

For high SE interaction energy, DP3 and DP2 become DCP3 and DCP2 canted phases (distorted canted P3 and P2 phases, respectively). In the absence of electron–lattice interaction (limit  $B/t \rightarrow \infty$ ), the CP3 phase present a continuous angular

degeneracy [14]. Now, this degeneracy is broken by the lattice distortion. Instead of the continuous degeneracy, only four set of angles inside each CP3 polaron were found [17]. For instance, DCP3 phase in Fig. 1 is a distorted canted phase with angles  $\theta$  and  $\theta$ . Spring displacements decrease when  $\theta \rightarrow \pi$ . The expected DP2–DCP3, DCP3–EAFU and DP2–EAFU phase transitions are also obtained for values of the SE interaction energy above the T–EAFU phase transition (see Fig. 1). Finally, the DCP2–EAFU phase transition occurs for high SE interaction energy  $JS^2/t > 0.2542$ . DCP2 phase becomes AFU (anti-ferromagnetic undistorted) in the limit  $JS^2/t \rightarrow \infty$ . In this phase each electron is trapped in a single site forming a Wigner crystallization. It is important to mention that the size chosen for the linear chain ( $N = 24$  sites), does not change the nature of the phases involved in the phase diagram.

In conclusion, we have studied the phase diagram resulting from the interplay between magnetic and electron–lattice interactions within an exchange model in one-dimensional systems



**Fig. 3.** EAFU + DP3 phase for four electrons ( $x = 0.167$ ) and  $JS^2/t = 0.14$  showing (a) spring displacements and (b) angles and charge distribution. Partial spin configuration snapshot is also shown.

using large Hund's energy and classical localized spins. For low SE interaction energy, our results show phase separation between a ferromagnetic distorted and anti-ferromagnetic undistorted phases, all electrons being inside the ferromagnetic region. For large SE interaction energy, in the whole range of electron concentration, we found phase separation between the AF undistorted phase and two-site distorted magnetic polarons. Each polaron contains one electron and a Wigner crystallization can be identified. The important magneto-elastic effect obtained here leads to a lattice contraction that consequently change the lattice parameters. This lattice contraction can be related to the contraction of the rungs experimentally observed in the Fe-ludwigite [11].

**Acknowledgments**

We want to thank partial support from CONACyT Grant-57929 and PAPIIT-IN108907 from UNAM. E.V. thank DGAPA-UNAM for financial support.

**References**

- [1] See, for example, T.A. Kaplan, S.D. Mahanti (Eds.), *Physics of Manganites*, Kluwer Academic, Plenum Publisher, New York, 1999.
- [2] C.D. Batista, J. Erodes, M. Avignon, B. Alascio, *Phys. Rev. B* 62 (2000) 15047.
- [3] E. Carvajal, O. Navarro, R. Allub, M. Avignon, B. Alascio, *Eur. Phys. J. B* 48 (2005) 179; O. Navarro, B. Aguilar, E. Carvajal, M. Avignon, *J. Magn. Magn. Mater.* 316 (2007) e496.
- [4] C. Zener, *Phys. Rev.* 82 (1951) 403; C. Zener, *Phys. Rev.* 81 (1951) 440.
- [5] G.H. Jonker, J.H. Van Santen, *Physica* 16 (1950) 337; J.H. Van Santen, G.H. Jonker, *Physica* 16 (1950) 599.
- [6] P.W. Anderson, H. Hasegawa, *Phys. Rev.* 100 (1955) 675.
- [7] P.G. de Gennes, *Phys. Rev.* 118 (1960) 141.
- [8] E. Vallejo, M. Avignon, *Phys. Rev. Lett.* 97 (2006) 217203; E. Vallejo, M. Avignon, *Rev. Mex. Fis.* 53 (2007) 1; E. Vallejo, M. Avignon, *J. Magn. Magn. Mater.* 310 (2007) 1130.
- [9] M. Mir, et al., *Phys. Rev. Lett.* 87 (2001) 147201.
- [10] P.G. Radaelli, et al., *Phys. Rev. B* 49 (1994) 6239.
- [11] M. Mir, J. Janczak, Y.P. Mascarenhas, *J. Appl. Cryst.* 39 (2006) 42.
- [12] D.J. Garcia, et al., *Phys. Rev. Lett.* 85 (2000) 3720; D.J. Garcia, et al., *Phys. Rev. B* 65 (2002) 134444.

- [13] S. Yunoki, et al., *Phys. Rev. Lett.* **80** (1998) 845;  
E. Dagotto, et al., *Phys. Rev. B* **58** (1998) 6414.
- [14] E. Vallejo, F. López-Urías, O. Navarro, M. Avignon, *J. Magn. Magn. Mater.* **320** (2008) e425.
- [15] W. Koshibae, M. Yamanaka, M. Oshikawa, S. Maekawa, *Phys. Rev. Lett.* **82** (1999) 2119.
- [16] D.R. Neuber, et al., *Phys. Rev. B* **73** (2006) 014401.
- [17] E. Vallejo, *Microelectron. J.* **39** (2008) 1266.